

Finite Element Modelling of Titanium Foam Behaviour for Dental Application

Wiwat Tanwongwan and Julaluk Carmai , *Member, IAENG*

Abstract—The use of titanium foam (Ti-foam) as an implant material has gained a lot of interest recently due to its good biocompatibility as well as stable fixation between implant and human bone. A finite element model is required in order to effectively design appropriate implants. Accurate finite element analyses rely on accuracy and efficiency of the applied material models. Mechanical behaviour of the Ti-foam under loadings are different from the solid titanium therefore an appropriate metal foam constitutive model is needed. In this paper, the Deshpande and Fleck model which is available as the crushable foam model in the ABAQUS finite element software has been employed together with appropriate material parameters to describe the deformation behaviour of the Ti-foam with various porosity levels under compressive and bending loads. The simulation results have been compared against recently published data. Good comparisons have been seen. This validated Ti-foam material model has been employed to study stress distributions on the Ti-foam dental implant system.

Index Terms—Dental Implants, Finite element Analysis, Material model, Titanium foam

I. INTRODUCTION

Metal foams, a new class materials, have increasingly been employed for a range of applications such as structural components, automotive parts, sound and vibration absorbers, heat exchanger and biomedical implants [1]-[3]. This is due to their unique combination of properties such as low density, high specific stiffness, high specific strength and good energy absorption capability [4].

Among metal foams, titanium foams (Ti-foams) are preferred in many crucial applications including biomedical implants which biocompatibility is required. The main interests for using cellular metals come from the increase of the friction coefficient between the implant and the surrounding bone. It allows mechanical interlocking of bone with the implant by substantial bone in-growth and better long term stability. Additionally, stiffness of the implants can be tailored by varying porosity to reduce the stress shielding effect [5], [6]. One of promising biomedical application of Ti-foams is in dental implants.

Finite element analysis has played an important role in designing of dental implants [7]-[11]. The success of the increasing use of the finite element method for analysing structures and components rests upon the accuracy and efficiency of the applied material models. Mechanical

behaviours of Ti-foam under loadings are different from the solid titanium. The Ti-foam is compressible material of which volume changes during the deformation while the solid titanium is incompressible material of which volume does not change. Hence, metal foams can yield under hydrostatic loading in addition to deviatoric loading. Furthermore, different levels of porosity in Ti-foam lead to different mechanical properties and failure mechanisms [11]-[13]. An appropriate metal foam constitutive model is required in simulation using the finite element technique. Constitutive models for metal foams [14]-[17]. have been developed for the past decade. Some of them have been built in commercial finite element packages such as LS-DYNA and ABAQUS. Most of them have been applied successfully in describing behaviour of aluminium foam. However, very few have been employed for Ti-foam under complex loading conditions. This paper, therefore, addresses an examination of applicability of the Deshpande and Fleck model, which is available in the ABAQUS finite element package as the crushable foam material model, on describing the Ti-foam behaviour. It will be employed to study the stress distribution on the Ti-foam dental implant which is subjected to the complex stress states.

II. METAL FOAMS

A. Mechanical Behaviours of Metal Foams

The major difference between foam materials and solid materials is their microstructure. A large amount of cells or pores are present in metal foams can be imagined as sponge. A metal foam is, therefore, characterised microstructurally by its cell topology, relative density, cell size and cell shape [18]-[20]. The term, porosity, is a parameter used at the macroscopic scale to indicate the proportion of porous area in foams. The microstructure features of cellular metals are affecting their mechanical responses. The stress-strain curve for a metal foam in compression is characterised by three regimes *a linear elastic* regime, corresponding to cell bending or face stretching; *a stress plateau* regime, corresponding to progressive cell collapse by elastic buckling or plastic yielding; and *densification* regime, corresponding to collapse of the cell throughout the material and subsequent loading of cell edges and faces against one another. Low relative density metal foam can be deformed up to large strain before densification occurs [21]. For successful application as functional components, knowledge of the plastic yield surface and subsequent plastic flow behaviour of a metal foam is very important. In contrast to solid metals, metal foams can yield under hydrostatic loading in addition to deviatoric loading [4]. Therefore, the

Manuscript received Mar 04, 2011; revised April 1, 2011.

Wiwat Tanwongwan is with the faculty of Engineering King Mongkut's University of Technology North Bangkok. 1518 Piboolsongkram Rd Bangkok, Thailand (email: misterwiwat@yahoo.com)

Julaluk Carmai* is with the faculty of Engineering King Mongkut's University of Technology North Bangkok. 1518 Piboolsongkram Rd Bangkok, Thailand. (phone:662-9132500 ext 8208; fax 662-5870029; email: jcm@kmutnb.ac.th)

yield criterion depends on both the von Mises equivalent stress and the mean stress.

A number of experiments have been conducted to study the mechanical behaviour of aluminium foams and titanium foams. [1], [2], [11], [12], [18], [19], [22]. Imwinkelried [12], in particular, experimentally studied mechanical properties of open-pore Ti-foams produced using the space holder method. Ti-foams with 100-500 μm pores and with porosities of 50-80% were studied. Four types of tests included the static compression, tension, bending, torsion, cyclic compression and permeability. The Ti-foam used in the tests was found to be anisotropic. From all the tests, Imwinkelried [12] has concluded that porosity level affects the strength of materials. The Ti-foams are stronger perpendicular to the compaction direction and weaker along compaction axis. Such material is best used in compression, where structural integrity is guaranteed up to large plastic deformations. The typical yield strength of titanium foam with 62% porosity is above 60 MPa in compression, bending and tension. Stiffness values vary with the testing method from 7-14 GPa.

B. Material Models for Metal Foams

Since metal foam behaviours are different from that of solid metal, classical plastic theory cannot be used to describe their behaviours. A number of constitutive models have been developed. Yield surface depends on both the mean stress and the von Mises equivalent stress. All of them are phenomenological models. Schreyer, Zuo and Maji [14] developed a metal foam constitutive model which took into account an isotropy by introducing initial kinematics hardening in the yield criterion. The model of Schreyer is suitable for cyclic loading [22]. The model of Miller [15] based on modification of the Drucker-Prager yield criterion and introduced three adjustable parameters to fit the yield surface to the available experimental data. The deformation behaviours under compressive loading are not equal to those under tensile loading.

Deshpande and Fleck [16] developed a 3D model primarily based on the experimental tests of Al-foam, which has been built in the finite element package ABAQUS [23]. The model assumes similar behaviours in tension and compression hence isotropic hardening. Among these, the model developed by Deshpande and Fleck [16] has the simplest expression and has found wide-spreading applications. In this paper, the crushable foam model with isotropic hardening will be employed. The thorough validation of constitutive models appears to be needed. In the crushable foam model, the contribution of the mean stress on the yield function is realised through a material parameter known as a *shape factor*. It defines the aspect ratio of the elliptical stress. This shape factor quantitatively distinguishes the plastic behaviour of metal foams from solid metals. The yield function (Y) is given by

$$Y = \sqrt{q^2 + \alpha^2 p^2} - B \quad (1)$$

where q is the von Mises equivalent stress and p is the mean stress. B defines the size of the yield ellipse and is given in (2)

$$B = \alpha p_c = \sigma_c \sqrt{1 + (\alpha/3)^2} \quad (2)$$

p_c is the yield strength in hydrostatic compression. σ_c is the absolute value of the yield strength in uniaxial compression. α is a shape factor of the yield surface is given in (3).

$$\alpha = \frac{3k}{\sqrt{9 - k^2}} \quad (3)$$

and k is the ratio of initial yield stress in uniaxial compression and initial yield stress in hydrostatic compression. Equation (1) represents an elliptical yield surface in the stress plane of von Mises stress versus the mean stress as illustrated in figure 1.

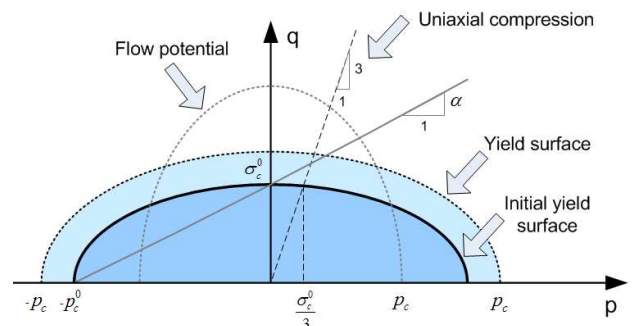


Fig.1. Yield surfaces and flow potential for the isotropic hardening crushable foam model.

The flow potential for the isotropic hardening model is chosen as

$$G = \sqrt{q^2 + \beta^2 p^2} \quad (4)$$

$$\beta = \frac{3}{\sqrt{2}} \sqrt{\frac{1 - 2\nu_p}{1 + \nu_p}} \quad (5)$$

ν_p is the plastic Poisson's ratio given by

$$\nu_p = \frac{3 - k^2}{6} \quad (6)$$

The plastic strains are

$$\dot{\epsilon}^{pl} = \dot{\lambda} \frac{\partial G}{\partial \sigma} \quad (7)$$

$\dot{\lambda}$ is the nonnegative plastic flow multiplier.

The elastic behaviour can be modeled only as linear elastic. The Young's modulus E_f has to be the one for metal foam which depends on the foam porosity.

III. SELECTION OF TI-FOAM MATERIAL PARAMETERS AND VALIDATION OF CONSTITUTIVE MODEL

Material parameters required for the crushable foam model are the Young's modulus (E), the yield strength of the Ti-foam (σ_y), the shape factor (α), the compressible yield stress ratio (k), the elastic and plastic Poisson's ratio (ν , ν_p) as well as hardening relation. The plastic Poisson's ratio was selected to reflect the shape of the workpiece during deformation. The parameters k and α were calculated from (3) and (6). The strategy was to use information from experimental data of Imwinkelried [12] for initial calibration and validation of the crushable foam model. Then the model was used to predict the mechanical behaviour of the Ti-foam at other levels of porosity during compression and bending.

A. Numerical Simulation of Compression Tests

A compression test of a 62.5% porosity Ti-foam cylinder with 8 mm diameter and 16 mm height as shown in figure 2 was simulated to test the accuracy of the crushable foam model in capturing the mechanical behaviour of the Ti-foam. The upper flat die moved down 0.8 mm with strain rate of 0.005 s^{-1} while the lower flat die was fixed. The dies were modeled as rigid surfaces. Axisymmetric elements were employed for the cylindrical workpiece. The friction coefficient between the contact surfaces was set to be 0.5 [24].

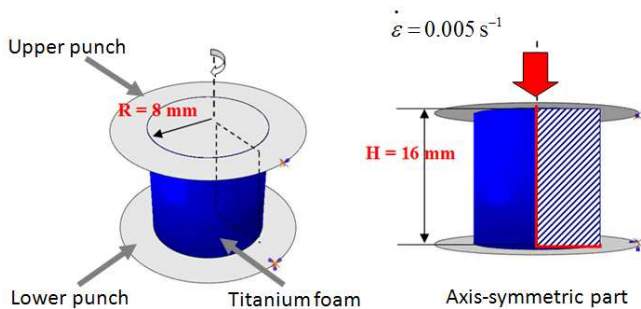


Fig. 2. Cylindrical specimen for simulations of compression tests.

The Young modulus (E) and the yield stress (σ_y) of 62.5% porosity Ti-foam were calculated using (8) and (9) which obtained from the experiments of Imwinkelried [12].

$$E = E_s(-0.024 + 15.86 \rho_r^2) \quad (8)$$

$$\sigma_y = (\sigma_y)_s(-0.068 + 7.684 \rho_r^{\frac{3}{2}}) \quad (9)$$

where E_s is the Young's modulus of the fully solid titanium which was taken as 110 GPa for pure titanium grade 4 [12] and $(\sigma_y)_s$ is the yield strength of the fully solid titanium which was taken as 650 MPa. ρ_r represents relative density of the metal foam. it is linearly proportional to percent of porosity according to Imwinkelried's experimental data. The plastic Poisson's ratio (ν_p) was assumed to be 0.34 to reflect the shape of the specimen. The compressible stress ratio (k) was calculated from (6) as 0.98.

The average macroscopic stress-strain curve obtained from the simulation was calibrated against experimental results of Imwinkelried [12] as shown in figure 3 for Ti-foam with 62.5% porosity. Good comparison can be seen especially at the *stress plateau* regime.

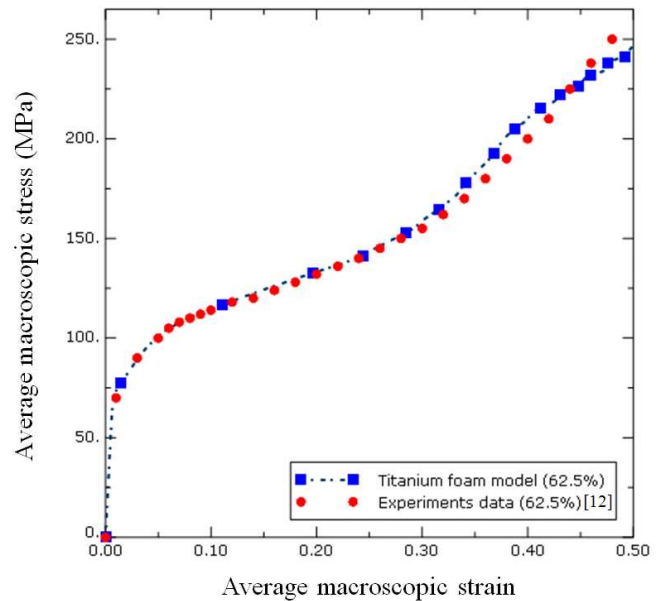


Fig. 3. Graph showing a comparison of average macroscopic stress-strain curves obtained from the experiment [12] and the simulation.

Figure 4 shows a comparison of deformed profiles of the specimen obtained from the experimental results [12] and the simulation. The deformed profiles obtained from the simulation compare well with those obtained from the experiment.

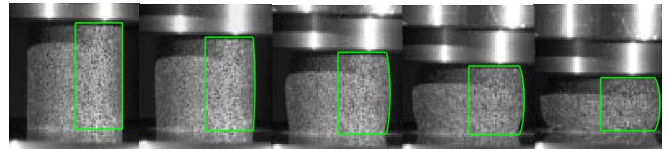


Fig. 4. shows profile shape of the specimen at various stages of deformation obtained from both the experiment [12] and the simulation.

Contour plot of von Mises stress of the compressed Ti-foam is shown in figure 5.

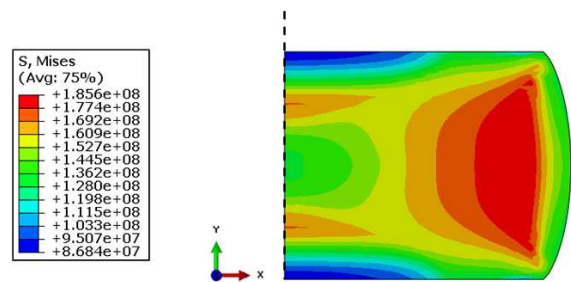


Fig. 5. shows distribution of the von Mises stress on the specimen.

The stress distribution is non-uniform with stress gradient around 53%. The maximum equivalent stress is found near the bulge area. The minimum equivalent stress is found at

the top and bottom of the specimen. Shear band is seen on the specimen at which the failure could be observed.

Equations (6), (8) and (9) with v_p of 0.34 were employed to predict the mechanical behaviour of Ti-foam at 59.9% and 65% porosity. The comparisons of experimental results and the simulations are shown in figure 6. It is possible to observe reasonable agreements between the numerical and the experimental curves, in particular at the *stress plateau* regime. The discrepancy is seen clearer at the *densification* regime where density is increasing. The comparison shows that the Deshpande and Fleck model in ABAQUS with the selected parameters for Ti-foam can be used to describe the behaviour of the Ti-foam under compressive loading.

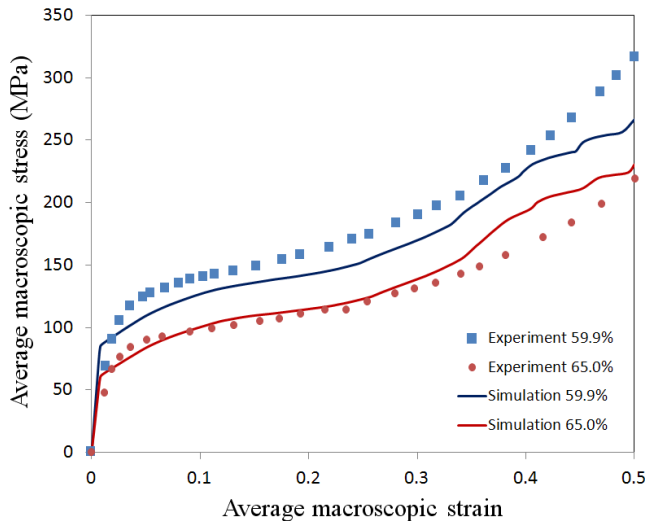


Fig. 6. showing average macroscopic stress-strain curves for Ti-foam with 65% and 59.9% porosity compared with experimental results by Imwinkelried [12].

B. Numerical Simulation of Three-point bending Test

The same material model as used in compression tests were employed to simulate the three-point bending test of 63.9% porosity of Ti-foam for comparison with the bending test of Imwinkelried [12]. Three dimensional model of the three-point bending test was constructed as shown in figure 7. The support rollers and the upper movable roller were modeled as analytical rigid bodies. The support rollers were fixed with 30mm distance in between. The width and the height of the specimen were 8.2 mm and 4.2 mm, respectively.

The movable roller moved down 1.5 mm. The specimen was meshed with the three dimensional solid continuum elements C3D8. The maximum bending stress was calculated using (10) [25].

$$\sigma_{bending} = \frac{3FL}{2BH^2} \quad (10)$$

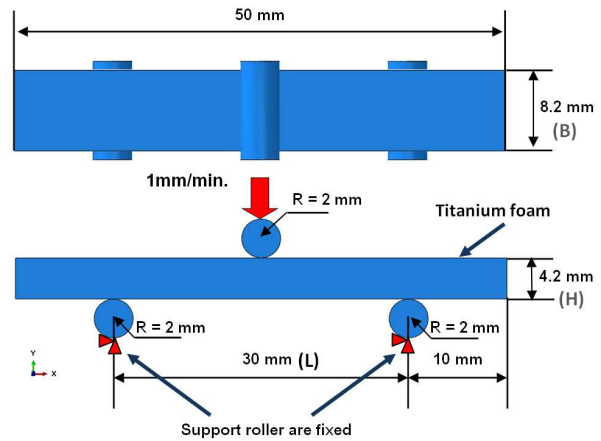


Fig. 7. Model set up for the three-point bending test.

Where F is the reaction force at the roller. L is the distance between the supports, B is width and H is the height of the specimen. The maximum bending stress obtained from the simulation at various displacements was plotted in figure 8 together with the experimental data of Imwinkelried [12]. The graph was plotted up to 0.8 mm as at 0.8 mm the first crack appeared within the specimen. The load then dropped. The softening was observed in the experiment. The bending stress trend is, therefore, predicted accurately up to nearly 0.8 mm because the model does not take into account the damage or failure criteria. The simulation compares well at small deflection. The discrepancy increases as the deflection approaching 0.8 mm.

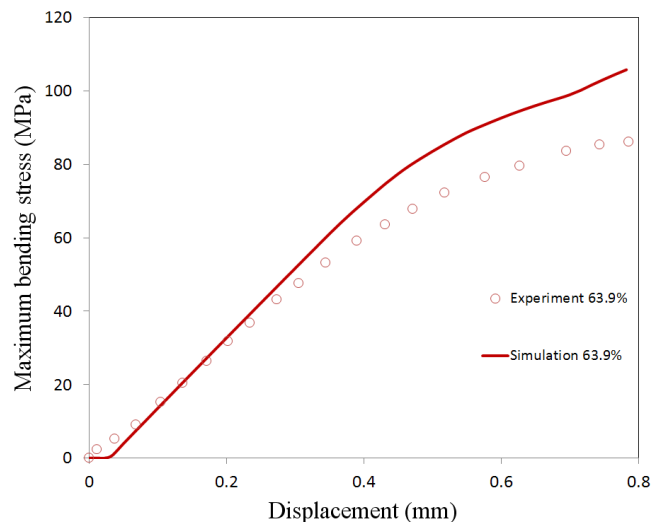


Fig 8. Showing graph of maximum bending stress versus displacement obtained from experimental data [12] and simulation.

The deformed shape of Ti-foam specimen with porosity of 62.5 % under the 3-point bending load is shown in figure 9. Stress is localized. Maximum equivalent stress occurs around bending region.

The Deshpande and Fleck model which was used to describe the deformation behavior of the Ti-foam was calibrated and validated with the experimental results. It was then employed to model the dental implant which is made from Ti-foam.

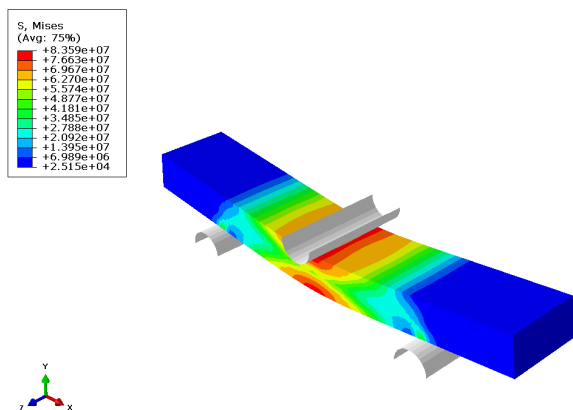


Fig. 9. Contour plot of von Mises stress on the bending specimen.

IV. APPLICATION OF TI-FOAM MODEL ON SIMPLE SHAPE OF DENTAL IMPLANT

The use of completely porous metals has the potential to solve the problems of fracture and stress shielding of bone. [5],[6]. To study the possibility of using Ti-foam as a dental implant, a three dimensional finite element analysis for Ti-foam dental implant system was carried out. And for comparison purpose a finite element model for solid titanium dental implant was also conducted.

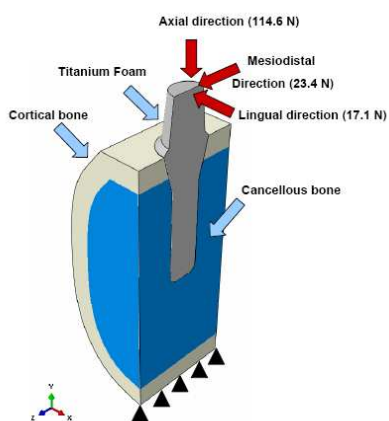


Fig. 10. The dental implant and surrounding bone system with applied loads and boundary conditions.

The three dimensional model of the dental implant and supporting bone system is shown in figure 10. The model consists of an implant and surrounding cancellous bone as well as cortical bone. Boundary conditions were applied to restrain all form of translational movements in the model. The interface between the implant and the bone as well as between the cortical and cancellous bone were treated as perfectly bond interface. Loading of the implant is shown in figure 10 with forces of 17.1 N, 114.6 N and 23.4 N in a lingual, an axial and mesio-distal direction [9]-[10]. Both cancellous bone and cortical bone assumed to be linear elastic [7]-[10]. The solid titanium assumed to be elastic-plastic. The material parameters of Ti-foam with 62.5% porosity were taken from section 4.

The material properties of the implant system of this study are summarised in Table I.

TABLE I
SUMMARY OF MATERIAL PROPERTIES USED IN THIS STUDY

Material	Young's modulus, E (GPa)	Poisson ratio (ν)	Yield stress (σ_y) (MPa)	Refs
Cortical bone	14.5	0.323	-	[7].
Cancellous bone	1.37	0.3	-	[7].
Titanium	110	0.3	650	[12].
Ti-foam* (62.5% porosity)	9.9	0.33	70	[12].

*The plastic Poisson ratio (ν_p) is 0.34 and the compressible yield stress ratio (k) is 0.98.

The finite element mesh was generated by using 3D solid continuum elements. The shape of implant was simplified as shown in figure 11.

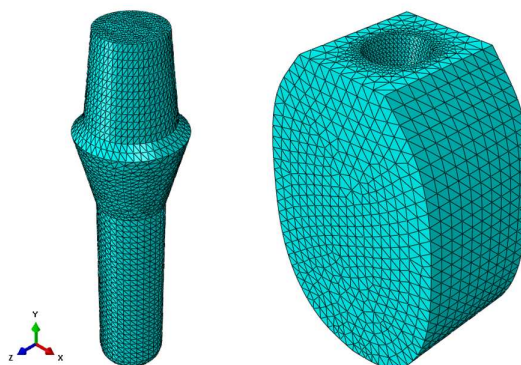


Fig. 11. The finite element mesh.

Two analyses were conducted one with the solid titanium implant and the other one with the Ti-foam implant. The stress distribution along both implants is inhomogeneous. Maximum equivalent stresses concentrated in the implants at the neck region. The level of stress within the Ti-foam implant is lower than that of the solid titanium implant as shown in figure 12.

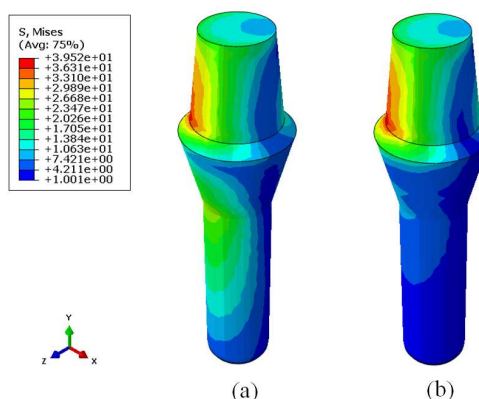


Fig. 12 represents the von Mises stresses distribution within (a) the solid titanium implant and (b) the Ti-foam implant.

Figure 13 presents level and distribution of equivalent stresses within the implant and surrounding bones. Stresses within the surrounding bones with the Ti-foam implant are a bit higher than the one with the solid titanium at around the neck region (area A in figure 13). It implies that more loads

can be transferred to the surrounding bones if the Ti-foam implant is used.

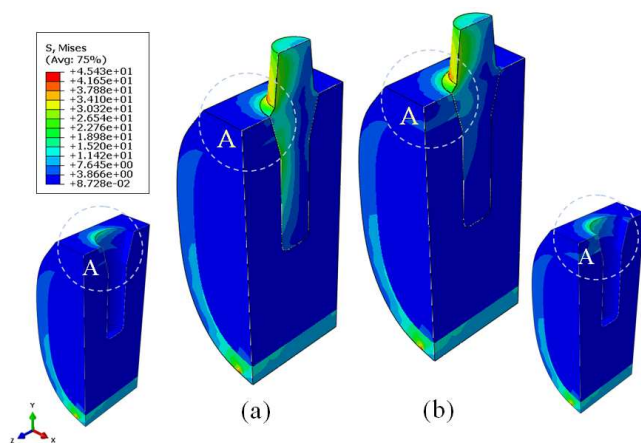


Fig. 13 showing the von Mises stress distribution within the surrounding bones as well as a) the solid titanium implant and b) the Ti-foam implant.

This is because the Ti-foam has lower stiffness than the solid titanium so the surrounding bone can share more load if the Ti-foam is used. The stresses in other parts are almost uniform hence shows little difference. This presents possibility to solve the stress shielding problem with Ti-foam implants. However, the present study is a simplified study. The real shape of implant and more complex interface condition must be considered to represent the real situation.

V. CONCLUSION

The Deshpande and Fleck model which is provided as the crushable foam model in the ABAQUS finite element software was employed to describe the behaviour of Ti-foam. The required material parameters were selected based on experimental data of Imwinkelried. The model was calibrated and validated against experimental data at various porosity levels for both compression and bending. Reasonable good agreements were obtained. The crushable foam model with calibrated parameters were then used in simulations of the dental implant system. The comparisons between the system with solid titanium implant and those with the Ti-foam implant were shown. The Ti-foam implant carried less stress than the solid titanium implant. However, the surrounding bone of the Ti-foam implant system carried more stress. This implies that more loads were transferred to the surrounding bone if the Ti-foam was used. Hence, stress shielding problem is possible to be solved. However, this study is a simplified study to show the applicability of using the Deshpande and Fleck model for the Ti-foam implant, the detailed study on design and optimization of the Ti-foam implant is required for further use.

REFERENCES

[1] L.J. Vendra and A. Rabiei, "Evaluation of modulus of elasticity of composite metal foams by experimental and numerical techniques," *Mat. Sci. Eng.* Vol 527, pp. 1784-1790, 2007.
[2] N. Tuncer and G. Arslan, "Designing compressive properties of titanium foams." *J. Mater. Sci.* vol 44 1477-1484, 2009.

[3] J. Banhart, "Manufacture characterisation and application of cellular metals and metal foams." *Progress in Materials Science*, pp. 559-632, 2001.
[4] M.F. Ashby, A.G. Evan, N.A. Fleck, L.J. Gibson, J.W. Hutchinson, H.N.G. Wadley, *Metal Foams : A Design Guide*. London : Butterworth-Heinemann, 2000.
[5] M.I. Z. Ridzwan and S. Shuib, "Problem of stress shielding and improvement to the hip implant designs." *J. Med. Sci.* vol 4, pp.460-467, 2007.
[6] W. Yan and C.L. Pun, "Spherical indentation of metallic foams," *Mater. Sci. Eng. A*, vol 527, pp. 3166-3175, 2010.
[7] A. Merdji, B. Bouiadjra, T. Achour, B. Seier, B. O. Chikh, and Z.O. Feng, "Stress analysis in dental prosthesis," *Com. Mater. Sci.*, vol 49, pp.126-133, 2010.
[8] J. Yang and HJ. Xiang, "A three-dimensional finite element study on the biomechanical behaviour of an FGBM dental implant in surrounding bone," *J. Biomech.*, vol 40, pp2377-2385, 2007.
[9] O. Kayabasi, E. Yuzbasioglu, and F. Erzincanli, "Static, dynamic and fatigue behaviors of dental implant using finite element method," *Adv. Eng. Soft.* Vol 37, pp.649-658, 2006.
[10] N. Djebbar, B. Serier, B. B. Bouiadjra, S. Benbarek, and A. Draï, "Analysis of the effect of load direction on the stress distribution in the dental implant," *Mater. Des.*, vol 31, pp. 2097-2101, 2010.
[11] H. Schiefer, M. Bram, H.P. Buchkremer, and D. Stover, "Mechanical examinations on dental implants with porous titanium coating," *J. Mater. Sci: Mater. Med.*, vol 20, pp. 1763-1770, 2009.
[12] T. Imwinkelried, T. "Mechanical properties of open-pore titanium foam," *J. Biomed Mater Res A*, pp. 964-970, 2007.
[13] S. Kashef, A. Asgari, T. B. Hilditch, W. Yan, V. K. Goel, and P. Hodgson, "Fracture toughness of titanium foams for medical applications," *Mater. Sci. Eng. A*, vol 527, pp. 7689-7693, 2010.
[14] H.L Schreyer, Q.H Zuo, A.K Maji, "Anisotropic plasticity model for foams and honeycombs" *J. Eng. Mech.* pp. 1913-1930, 1994.
[15] R. Miller, "A continuum plasticity model of the constitutive and indentation behavior of foamed metals," *Inter. J. Mech. Sci.* pp. 729-754, 1999.
[16] V.S. Deshpande, N. A. Fleck, "Isotropic constitutive models for metallic foams" *J. Mechs. Phys. Solids.* pp.2139-2150,2000.
[17] S. Shima, O. Oyane, "Plasticity Theory for Porous Metals." *Int. J. Mech. Sci.* vol 18, 285-291,1976.
[18] A. Nouri, A.B. Chen, P.D. Hodgson, and C.E. Wen, "Preparation and characterization of New Titanium Based Alloys for Orthopaedic and Dental applications," *Adv. Mater. Res.*, vol 15-17, pp.71-76, 2007.
[19] J. Bin, W. Zejun, and Z. Naiqin, "Effect of pore size and relative density on the mechanical properties of open cell aluminium foams," *Scripta. Mater.*, vol 56, pp.169-172, 2007.
[20] A.-F. Bastawros, H. Bart-Smith, and A.G. Evans, "Experimental analysis of deformation mechanisms in a closed-cell aluminum alloy foam," *J. Mech. Phys. Solids.*, vol 48, pp.301-322, 2000.
[21] L.J. Gibson and M.F. Ashby. *Cellular Solids: Structure and Properties*. 2nd ed. 1997, Cambridge University Press.
[22] A.G. Hanssen, O.S. Hopperstad and M. Langseth, "Validation of constitutive models applicable to aluminium foams," *Int. J. Mech. Sci.* pp. 359-406,2002.
[23] *Abaqus 6.9 Documentation Theory Manual*, Hibbit, Karlsson and Sorensen, 1998.
[24] Obert, R. et al. *Frictional Properties of BIOFOAM™ Porous Titanium Foam*. Wright Medical Technology, 5677 Airline Rd, Arlington, TN 38002.
[25] *ASM Handbook. Mechanical Testing and Evaluation*. Vol. 8, 2000.